FFEMS Fatigue & Fracture of Engineering Materials & Structures
ORIGINAL CONTRIBUTION
doi: 10.1111/ffe.12560

Analytical modelling of residual stress in additive manufacturing

O FERGANI[1], F BERTO[1], T WELO[1] and S Y LIANG[2]

[1]*Department of Mechanical and Industrial Engineering, NTNU—Norwegian University of Science and Technology, Trondheim, Norway,* [2]*Georges W. Woodruff School of Mechanical Engineering, Georgia Institute of Technology, Atlanta, GA, USA*

Received Date: 05 October 2016; Accepted Date: 07 November 2016; Published Online:

ABSTRACT A physics-based analytical model to assess residual stresses in additive manufacturing made of metallic materials is presented and validated experimentally. The model takes into consideration the typical multi-pass aspect of additive manufacturing. First, the thermal signature of the process is assessed by predicting the temperature for the problem of a moving heat source, then, the thermally induced stresses in a homogenous semi-infinite medium are determined. Taking the thermal stresses as input, the residual stresses are calculated analytically to obtain the distribution across the depth. Good agreement is obtained between the analytical prediction and X-ray measurements made on Selective Laser Melted 316L Stainless Steel. In addition, the analytical approach enables in-depth interpretations of results with basis in the true mechanisms of the process. Thus, the present model appears as a promising tool for optimization of process parameters in additive manufacturing, which in turn will improve the understanding of process parameters and their effect on properties of the final product.

Keywords additive manufacturing; analytical; residual stress; selective laser melting; steel 316L; X-ray measurement.

NOMENCLATURE

c = heat capacity (J/K)
E = elastic modulus (MPa)
R = Volumic heat capacity
G = bulk modulus (MPa)
G_{xh}, G_{zh}, G_{xzh}, G_{xy}, G_{zy}, G_{xzy} = plane strain Green's functions
h = plastic modulus (MPa)
h_e = enthalpy (J/kg)
k = conductivity (W/m K)
n_{ij} = components of unit normal in plastic strain rate direction
P_L = laser power (W)
r = radial distance from heat source (m)
r_0 = laser spot radius (m)
t = time (s)
T = temperature (C)
T_0 = room temperature (C)
T_m = melting temperature (C)
$\frac{\partial T}{\partial x}$, $\frac{\partial T}{\partial z}$ = temperature gradient
u = internal energy (J/kg)
V = scan speed (m/s)
x = coordinate along scan direction (m)
y = coordinate perpendicular scan direction (m)
z = coordinate in depth (m)
α = thermal diffusivity (m^2/s)

Correspondence: O. Fergani. E-mail: o.fergani@ntnu.no

$\Delta\sigma_{xx}, \Delta\sigma_{yy}, \Delta\sigma_{zz}, \Delta\tau_{xz}, \Delta\varepsilon_{xx}$ = stress increments (MPa)
$\dot{\varepsilon}_{xx}, \dot{\varepsilon}_{yy}, \dot{\varepsilon}_{zz}$ = strain rate
θ = dimensionless temperature
ν = Poisson's ratio
ρ = density (kg/m^3)
Ψ = hybrid function
$\varepsilon^r_{xx}, \sigma^r_{zz}, \tau^r_{xz}$ = residual stress components
$\sigma^{therm}_{xx}, \sigma^{therm}_{zz}, \sigma^{therm}_{xz}, \sigma^{therm}_{yy}$ = thermal stresses
$\dot{\sigma}_{xx}, \dot{\sigma}_{yy}, \dot{\sigma}_{zz},$ = stress increment of normal directions x, y and z
$\sigma^*_{xx}, \sigma^*_{zz}, \tau^*_{xz}$ = stress incremental form of the thermal elastic stresses

INTRODUCTION

Additive manufacturing processes are seen as a pillar of the next industrial revolution.[1] The societal impact of additive manufacturing technologies is substantial at different levels.[2] Nevertheless, the fundamental understanding of the interactions between process and materials is key to enhance product quality and accelerate the adoption of additive manufacturing in modern production systems. One of the challenges of additive manufacturing of metallic components in both powder-bed and powder deposition technologies is residual stress accurate knowledge. Residual stresses are the stresses that remain in the body after the thermo-mechanical processing is completed. They play an important role in the performance of a manufactured component (fatigue life, corrosion resistance, crack propagation, distortions, dimensional accuracy, etc.). Residual stresses are inherent to all manufacturing processes; occasionally, they can be beneficial with proper control, for example, generating compressive stresses in the surface and sub-surface layers of components. Serious challenges in additive manufactured components such as thermal cracks, distortions and tensile stresses in the surface layer are because of residual stresses. These defects create significant problems for manufacturing high-quality components in industry. When using laser-based manufacturing, the large energy density delivered by the laser creates substantial temperature gradients in the material. This non-uniform heating causes expansion and contraction that potentially may generate large residual stresses. Some of the first studies of this problem have already investigated the influence of bed heating on the formation of residual stresses. Surface and near surface layers are found to be under tension when produced using selective laser melting (SLM).[3] Also, the authors reported on the influence of the heating of the bases on the reduction of residual stresses. The authors also reported that heat treatment helped reduce the residual stresses by 70%. The build strategy or the scanning path is an important parameter to investigate. In a recent contribution,[4] a numerical approach is presented based on finite element to investigate the influence of the build strategy on the residual stress profile during SLM. The results suggest that in order to understand the intensity of the residual stress, the thermal load needs to be investigated. The length of the scanning track contributes directly to increase the thermal signature of the process and therefore the residual stresses. The authors presented an enhanced finite element model used to predict the residual stresses and induced distortions.[5] A comprehensive experimental study was recently conducted,[6] where distortions in build structure as well as residual stresses were measured using X-ray. According to the author, the developed model does not provide a fundamental representation of the underlying mechanism behind the formation of the residual stresses in SLM. However, these models suffer from large computational time and the lack of physical interpretation of the phenomena.[7,8] The authors investigated the sensitivity of residual stress to variation in materials properties. They found no clear evidence on a proven influence, consolidating the strong influence of the melting/solidification process on residual stresses. An empirical model to help interpret the origin of the residual stresses during the melting processes has been provided in a recent study.[7] The model provided insights based on experimental observations and a developed process map. Nevertheless, the study could not capture the fundaments of the formation of these stresses during the additive manufacturing process. Different research proposed comprehensive experimental investigation of the residual stress in the surface and the bulk of printed structures.[8,9] They report, mainly tensile residual stresses in the surface and subsurface. Based upon the review of the literature, and the increasing number of scientific publications on this topic, it appears that the understanding of residual stresses is substantial to achieve high performance components. Further, the fundamental understanding of the underlying physics at the origin of these residual stresses is additive manufacturing need to be introduced, and ultimately used to perform sensitivity studies and optimize process conditions. In this paper, we propose for the first time a framework of an analytical solution to model and assess the residual stresses in the

additive manufacturing of metallic components. The potential of the new solution can affect a wide range of applications becoming a powerful tool for the design and also for the fatigue assessment when the component is subjected to cyclic loading.

In the remainder of this paper, we propose a novel analytical model for prediction of residual stresses in the additive manufacturing of metallic components. In the next section, we introduce the analytical solution for the temperature induced by the laser, then the fundamental equation to calculate the thermal stresses and finally we tersely the residual stress prediction. In the subsequent section, the model is validated experimentally based on X-ray measurement using Selective Laser Melted 316L. Finally, the obtained results are presented and discussed.

ANALYTICAL MODEL

Temperature

The general convection–diffusion equation in the case of a moving heat source representative for the one in laser based additive technologies is formulated as

$$\frac{\partial \rho u}{\partial t} + \frac{\partial \rho h_e V}{\partial x} = \nabla \cdot (k \nabla T) + R \tag{1}$$

where u is the internal energy, h_e is the enthalpy, ρ is the density, k is the conductivity, R the volumetric heat source, T the temperature and V the relative speed difference between the heat source or the medium. The first and second terms on the left hand side in Eq. (1) represent the change of internal energy and convection, respectively. The corresponding terms on the right hand side are heat conduction and a heat source or sink. We assume a moving point heat source. The basic temperature equation is written as in Eq. (2)

$$\theta = \frac{P_L}{4\pi k r (T_m - T_0)} \exp\left(-\frac{V(r+x)}{2\alpha}\right) \tag{2}$$

where the dimensionless temperature $\theta = (T - T_0)/(T_m - T_0)$. According to this equation, the temperature becomes infinite at the heat source location. As a basis for solving the temperature equations, it will be assumed that the medium is homogenous, isotropic and semi-infinite. Moreover, the material's properties are temperature dependent. In this work, the temperature dependency of the properties of 316L is considered and adapted.[10] Based on the temperature prediction at each point of the plane, the temperature gradient is calculated. The outcomes of this section are used as input to calculate the thermal stresses induced by the non-uniform heating during the SLM process.

Thermal stresses

The non-uniform heating may lead to residual stresses, specifically when severe cooling rate are observed, specific to additive manufacturing. The amount of residual stresses and their nature depends on the thermal stresses experienced by the medium. In the case of additive manufacturing, only thermal stresses are observed and can be predicted using the temperature and temperature gradient knowledge. Timoshenko defined thermal stresses as a superposition of three individual stress components; namely, body forces induced by the temperature gradient, tension on the surface and hydrostatic pressure.[11] Further development in the understanding of the thermal stresses in the context of nonlinear elasticity can be found in recent reports.[12,13] Figure 1 shows the configuration of the model proposed in this paper. In the case of plane stress, and two-dimensional semi-infinite medium, the resulting thermal stresses are given as:

$$\begin{aligned}
\sigma_{xx}^{therm}(x,z) &= -\frac{\alpha E}{1-2\nu}\int_0^{\infty}\int_{-\infty}^{\infty}\left(G_{xb}\frac{\partial T}{\partial x}(x',z') + G_{xv}\frac{\partial T}{\partial z}(x',z')\right)dx'dz' \\
&\quad + \frac{2z}{\pi}\int_{-\infty}^{\infty}\frac{p(t)(t-x)^2}{\left((t-x)^2+z^2\right)^2}dt - \frac{\alpha E T(x,z)}{1-2\nu} \\
\sigma_{zz}^{therm}(x,z) &= -\frac{\alpha E}{1-2\nu}\int_0^{\infty}\int_{-\infty}^{\infty}\left(G_{zb}\frac{\partial T}{\partial x}(x',z') + G_{zv}\frac{\partial T}{\partial z}(x',z')\right)dx'dz' \\
&\quad + \frac{2z^3}{\pi}\int_{-\infty}^{\infty}\frac{p(t)}{\left((t-x)^2+z^2\right)^2}dt - \frac{\alpha E T(x,z)}{1-2\nu} \\
\sigma_{xz}^{therm}(x,z) &= -\frac{\alpha E}{1-2\nu}\int_0^{\infty}\int_{-\infty}^{\infty}\left(G_{xzb}\frac{\partial T}{\partial x}(x',z') + G_{xzv}\frac{\partial T}{\partial z}(x',z')\right)dx'dz' \\
&\quad + \frac{2z^2}{\pi}\int_{-\infty}^{\infty}\frac{p(t)(t-x)}{\left((t-x)^2+z^2\right)^2}dt \\
\sigma_{yy}^{therm}(x,z) &= \nu\left(\sigma_{xx}^{therm} + \sigma_{zz}^{therm}\right) - \alpha E T(x,z)
\end{aligned} \tag{3}$$

where,

$$p(t) = \frac{\alpha E T(x, z=0)}{1-2\nu} \tag{4}$$

and $(G_{xb}, G_{zb}, G_{xzb}, G_{xv}, G_{zv}, G_{xzv})$ are the plane-strain Green's functions. The Green's functions are derived in a previous work,[14] providing an analytical solution to a thermal shear stresses in the case of non-uniform heating on an interface.

At this point, the additive manufacturing process signature, defined as the physical condition to which a material is subject to, at different scales is calculated analytically. The thermal load is defined here as the temperature, heating and cooling rate, the temperature

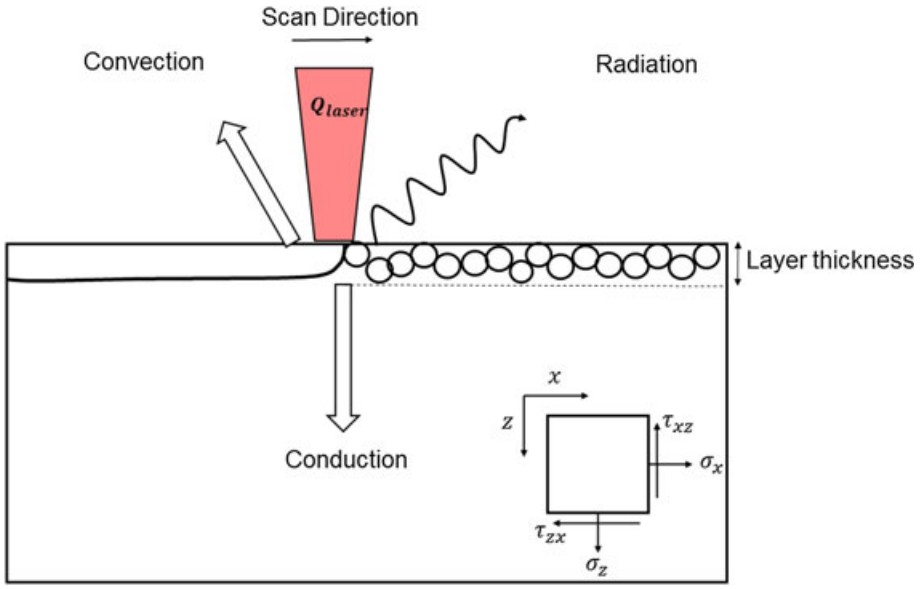

Fig. 1 Plane stress configuration with the heat input and the coordinates.

gradient in the bulk and the induced thermal stresses. The residual stresses in a solid built using additive manufacturing are predicted using the framework presented in the next section. The model takes as input the calculated thermal stresses in Eq. (3).

We introduce,

$$\begin{aligned} &\sigma_{xx}^{*} = \sigma_{xx}^{therm},\ \sigma_{zz}^{*} = \sigma_{zz}^{therm} \\ &\tau_{xz}^{*} = \sigma_{xz}^{therm}. \end{aligned} \tag{5}$$

Residual stresses

Laser-based thermal or thermo-mechanical treatments are known to be a common source of large residual stresses. This is because of the non-uniform heating in terms of contraction and extension of the material. Another source of residual stress is the difference in the thermal expansion coefficient between different phases for the same materials. Residual stresses can also be the result of the chemical composition gradient within a workpiece of the same material. It is worth mentioning that residual stresses can be theoretically eliminated by designing controlled cooling processes to achieve a full relaxation of the residual stresses. However, this is a very hard task practically, although more and more additive manufacturing processes are using a heated platform for that purpose.

A model enabling the prediction of subsurface cyclic plasticity and residual stresses for loading conditions ranging from small to large cyclic plastic-strain ranges was introduced.[15] The model presented in Eq. (6) considers the cyclic plastic flow and the resulting residual stresses. We assume a cycle as a deposition of a layer. The model takes as input the thermal stresses Eq. (3) calculated using the temperature, temperature gradient Eq. (1) and the material properties. The stress increment in the build direction and in the perpendicular direction can be found by solving the system of equations proposed below,

$$\begin{cases} \dot{\varepsilon}_{xx} = \dfrac{1}{E}\left[\dot{\sigma}_{xx} - \nu\left(\dot{\sigma}_{yy} + \dot{\sigma}_{zz}\right)\right] + \dfrac{1}{h}\left(\dot{\sigma}_{xx}n_{xx} + \dot{\sigma}_{yy}n_{yy} + \dot{\sigma}_{zz}n_{zz} + 2\dot{\tau}_{xz}^{*}n_{xz}\right)n_{xx} \\ = \Psi\left(\dfrac{1}{E}\left[\dot{\sigma}_{xx}^{*} - \nu\left(\dot{\sigma}_{yy} + \dot{\sigma}_{zz}^{*}\right)\right] + \dfrac{1}{h}\left(\dot{\sigma}_{xx}^{*}n_{xx} + \dot{\sigma}_{yy}n_{yy} + \dot{\sigma}_{zz}^{*}n_{zz} + 2\dot{\tau}_{xz}^{*}n_{xz}\right)n_{xx}\right) \\ \dot{\varepsilon}_{yy} = \dfrac{1}{E}\left[\dot{\sigma}_{yy} - \nu\left(\dot{\sigma}_{xx} + \dot{\sigma}_{zz}^{*}\right)\right] + \dfrac{1}{h}\left(\dot{\sigma}_{xx}n_{xx} + \dot{\sigma}_{yy}n_{yy} + \dot{\sigma}_{zz}n_{zz} + 2\dot{\tau}_{xz}^{*}n_{xz}\right)n_{yy} = 0 \\ \dot{\sigma}_{yy} = \dfrac{1}{2}\left(\dot{\sigma}_{xx} + \dot{\sigma}_{zz}\right) \end{cases} \tag{6}$$

where E is the elastic modulus, Ψ is the blending function and ν is the Poisson ratio. $\dot{\sigma}_{xx}$, $\dot{\sigma}_{yy}$, $\dot{\sigma}_{zz}$ are the stress increment of normal directions x, y and z. $\dot{\sigma}^*_{xx}$, $\dot{\sigma}^*_{zz}$, $\dot{\tau}^*_{xz}$ are the incremental form of the thermal stresses Eq. (5). In order to implement this model, compatibility requirement and boundary conditions are maintained. In the model used herein, the elasto-plastic relationship between the three normal stresses is written in incremental form and added to the residual stress model. The utilized model is an enhanced algorithm for residual stress predictions thanks the to the incorporated hybrid function as a limiting case for very large and very small plastic strain range.

$$\Psi = 1 - \exp(-\kappa(3h/2G)) \tag{7}$$

where E is Young's modulus and G is the bulk modulus. Because the strain rate in the traverse direction is zero because of the assumption of plane strain,

During the build procedure, the workpiece undergoes non-proportional cyclic plastic deformation induced by the heat from the successive laser scans. To capture this behaviour, a multiple back-stress nonlinear dynamic recovery constitutive law is integrated to capture the cyclic plasticity generated by the additive manufacturing process.

The stress relaxation starts when the temperature decreases to the ambient temperature, as a new state of stress and strain exist in the bulk of the materials. Based on the stress invariant assumption, this distribution does not correspond to the actual residual stress and strain distribution. After a relaxation of M steps (100 to 1000), the nonzero components ε^r_{xx}, σ^r_{zz}, τ^r_{xz} are reduced to incrementally to zero after each pass as described in Eq. (8)

$$\begin{aligned} \Delta\sigma_{zz} &= \frac{\sigma^r_{zz}}{M}, \\ \Delta\tau_{xz} &= \frac{\tau^r_{xz}}{M}, \\ \Delta\varepsilon_{xx} &= \frac{\varepsilon^r_{xx}}{M} \end{aligned} \tag{8}$$

EXPERIMENTS AND VALIDATIONS

The developed model is validated in the case of SLM of 316L Stainless Steel. The nominal chemical composition (in wt%) is presented in Table 1. The powder size distribution is characterized as, $d_{10} = 3.0\ \mu m$, $d_{50} = 7.1 \mu m$ *and* $d_{90} = 27.5 \mu m$. The 316L samples are produced using a Phenix PM100 system. The laser beam had a TEM_{00} Gaussian profile with 70 μm port size diameter. The laser power was 50 W, and the scanning speed was 0.1 m/s. The samples of $3 \times 3\ cm^2$, 1 layer, 5 layers and 25 layers with 50 μm layer thickness, were manufactured using a one-direction scanning with a hatch distance of 70 μm. The build strategy consisted in parallel tracks repeated in each new layer is shown in Fig. 2. The complete experimental setup details can be found in a recent contribution.[16]

RESULTS AND DISCUSSION

The presented model is implemented computationally. The moving heat source for the case of a point heat source is computationally solved using Matlab. Figure 3 shows the temperature distribution obtained in the scanning direction for one track. The results show elongation of the melt pool and the heat-affected zone (HAZ), which is typical for additive manufacturing. It also shows the temperature peak obtained in the simulated case of 2500 °C. The model predicted the temperature at every point of the surface and subsurface. The temperature dependence of the physical properties such as the thermal conductivity and expansion coefficient is considered based on some previous data reported.[10] Large residual stresses are expected to develop in the vicinity of the dif-

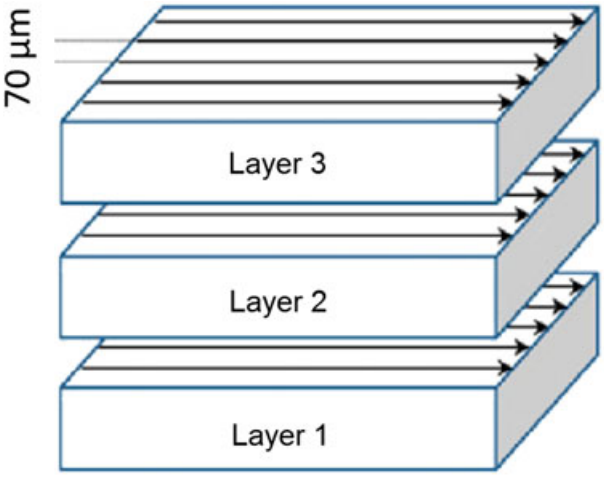

Fig. 2 Build strategy for 316L samples [14].

Table 1 Chemical composition of 316L (wt%)

Fe	Cr	Ni	Mo	Mn	Si	C	P	Cu	N
Balance	17.5–18	12.5–13	2.25–2.5	Max 2	Max 0.75	0.03	0.025	0.5	0.1

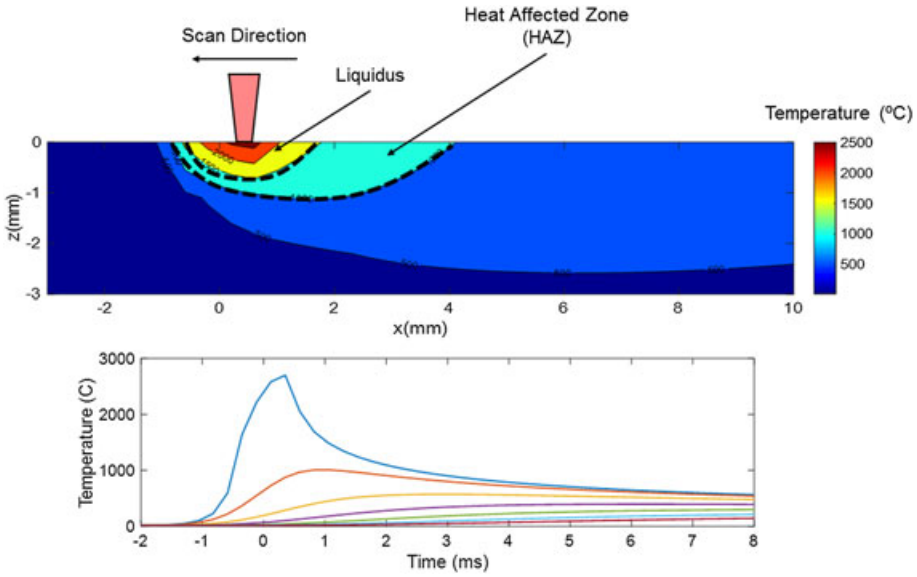

Fig. 3 Temperature (°C) distribution in 2D during the laser melting of the power, the heating rate at different depths of the additive manufactured layers.

ferent melted tracks starting from a stress free state in the molten metal at peak temperature. In additive manufacturing of 316L, the values of the generated residual stresses are higher than the reported wrought yield strength (500 MPa) in an area up to a depth between 150 µm and 200 µm. Considering the iterative nature of laser melting in additive manufacturing, a scheme of heating and subsequent cooling generates a complex residual stresses profile. In the case of multi-layers, the magnitude of the residual stresses depends on the different cooling rate in the depth of the sample.

The proposed analytical model considers the influence of multi-loading on the predicted residual stresses profile. Similar approach has been described in previous work by the authors for the case of residual stress regeneration in milling.[17] The objective is to capture the influence of the existing residual stress profile on the new state resulting from the subsequent loading. In this study, the residual stress in different configuration of multi-passes layer additive manufacturing is considered. The in-depth profile of residual stresses is predicted for the case of one pass, 5 passes and 25 as shown in (Figs 4–6).

Predicted residual stresses in the surface and subsurface are in tension in coherence with most of the reported results in the literature. The residual stress profile is assessed only for the first layers of the structure (up to 30 µm) where the influence of the process signature is dominant in terms of residual stress generation. The objective is to avoid the mismatch because of the connection with the build plate where a transition from tensile to compressive is expected. The model was calibrated using the hybrid function as the only adjustable parameters ($\psi = 0.15$) in order to fit the obtained results in the case

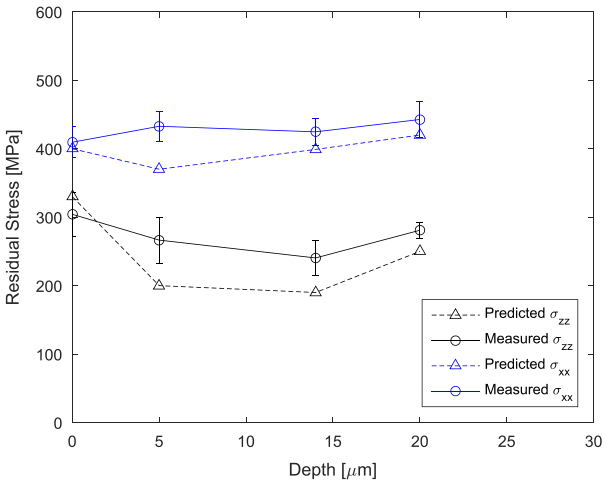

Fig. 4 Predicted and measured residual stress in both build and orthogonal to build direction for the case of one layer.

of one pass at the surface ($z = 0$) for σ_{zz}; the relaxation steps are set to $M = 100$. The temperature profile is in sound agreement with the simulated profile.[16] During the melting of a single layer, the residual stresses in the scanning direction are found to be higher than in the orthogonal direction (Fig. 4). We confirm similar observations for the cases of 5 and 25 passes (Figs 5 and 6). This is mainly because of the influence of the scanning speed on the melt pool shape and therefore the direction of cooling rate. This shows the influence of the scanning speed and direction on the residual stress directionality.

The experimental results show that increasing the number of scanning passes tends to reduce the average magnitude of residual stresses in both directions. This is

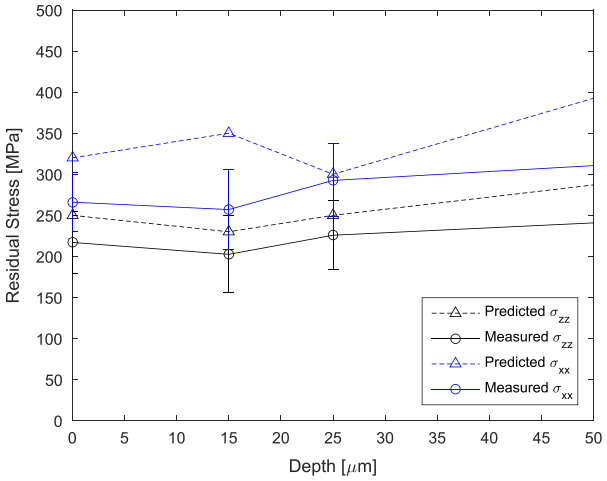

Fig. 5 Predicted and measured residual stress in both build and orthogonal to build direction for the case of 5 passes.

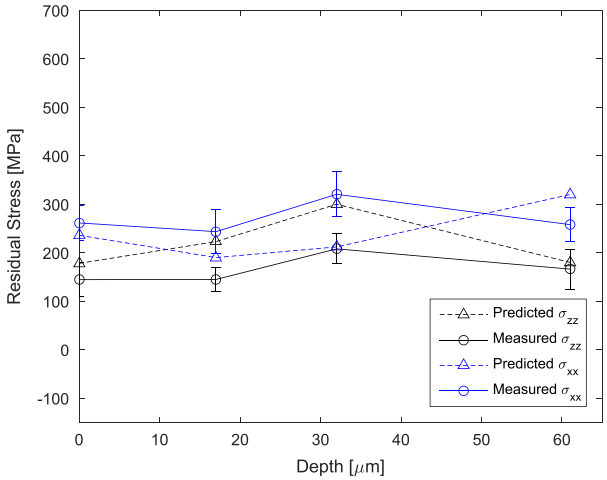

Fig. 6 Predicted and measured residual stress in both build and orthogonal to build direction for the case of 25 passes.

mainly because of the role of the heat affected zone (HAZ), as source of heat after the cooling process. The HAZ plays the role as energy source for a continuous relaxation of residual stress acting like a stress relief heat treatment. This is comforted by the actual usage of heated powder bed or build support as a mean to reduce residual stresses in previous studies.[8]

The novel analytical model was capable of predicting the nature and the average value of residual stress in the subsurface both scanning and orthogonal to scanning directions. The influence of the multi-passes is implemented and showed a capability to generate results in good agreement with the X-ray measurements. The model over predicted the surface residual stresses in some cases. This can be because of several factors: First, the complex heat transfer modes happening at the melted surface, which can lead to inaccurate prediction of the temperature on the surface and therefore the residual stresses. The second is the nature of heat conduction in a continuum homogenous medium, compared to the reality of the obtained samples with defects (pores, crack, etc.) inherent to additive manufacturing technology. Finally, inaccuracies arising from the X-ray measurement because of oxide layers forming immediately after the end of the additive process can be a cause of deviation between experimental and analytical results. The model will be improved considering these aspects. The predictive modelling of the residual stresses is key to predict the functionalities of the components in fatigue and fracture and can be compared to the results reported in some recent papers.[18–20] Based on this discussion, it is clear that powder-bed laser-melting and powder deposition processes are prone to induce tensile residual stress in the surface and subsurface on the components on the top of the different types of defect that are inherent to additive manufacturing. Hence, a post processing of the surface is required to achieve the desired surface integrity. The association of additive manufacturing to other nontraditional subtractive processes or cold deformation seems to be the path to follow to obtain structural integrity. The resulting surface integrity in the hybrid processes, where both additive and subtractive manufacturing are integrated is a promising research area.[21,22]

CONCLUSIONS

In this work, it has been introduced for the first time, a new analytical model to assess the residual stresses in additive manufacturing components. The model has been built based on successive predictions of the temperature profile, the thermal stresses and finally the residual stresses. The proposed model is capable of capturing the multi-loading aspects of the additive manufacturing processes. The model is validated by means of reported results on residual stresses in the SLM of 316L. The model assessments are compared to the obtained accurate X-ray measurements. The obtained results showed a good agreement with the experimental results. The nature of residual stresses has a tensile nature and is always higher in the scanning direction. This shows that the selection of the adequate scanning strategy can lead to an optimal residual stress profile. The increase of number of passes induced a larger HAZ. Observation showed that the HAZ plays a key role of an energy source for the thermal relaxation after the cooling phase is finished. The larger the HAZ, the lower are the average residual stresses in magnitude.

REFERENCES

1 Rifkin, J. (2012) The third industrial revolution: how the internet, green electricity, and 3-d printing are ushering in a sustainable era of distributed capitalism. *World Finan. Rev.*, **1**, 4052–4057.

2 Huang, S. H., Liu, P., Mokasdar, A. and Hou, L. (2013) Additive manufacturing and its societal impact: a literature review. *Int. J. of Adv. Manuf. Tech.*, **67**, 1191–1203.

3 Shiomi, M., Osakada, K., Nakamura, K., Yamashita, T. and Abe, F. (2004) Residual stress within metallic model made by selective laser melting process. *CIRP Ann. Manuf. Technol.*, **53**, 195–198.

4 Li, C., Fu, H., Guo, Y. B. and Fang, F. Z. (2016) A multiscale modeling approach for fast prediction of part distortion in selective laser melting. *J. Mater. Proces. Tech.*, **229**, 703–712.

5 Li, C., Liu, J. F. and Guo, Y. B. (2016) Prediction of residual stress and part distortion in selective laser melting. *Procedia CIRP*, **45**, 171–174.

6 Zaeh, M. F. and Branner, G. (2010) Investigations on residual stresses and deformations in selective laser melting. *Prod. Eng.*, **4**, 35–45.

7 Vasinonta, A., Beuth, J. L. and Griffith, M. (2007) Process maps for predicting residual stress and melt pool size in the laser-based fabrication of thin-walled structures. *J. Manuf. Sci. Eng.*, **129**, 101–109.

8 Brice, C. A. and Hofmeister, W. H. (2013) Determination of bulk residual stresses in electron beam additive-manufactured aluminum. *Metall. Mater.Trans. A*, **44**, 5147–5153.

9 Wu, A. S., Brown, D. W., Kumar, M., Gallegos, G. and King, W. E. (2014) An experimental investigation into additive manufacturing-induced residual stresses in 316L stainless steel. *Metal. Mater. Trans. A*, **45**, 6260–6270.

10 1999. Material Properties for Design) *IGCAR Data Book*. Kalpakkam, Tamil Nadu, India.

11 Timoshenko, S. P. and Gere, J. M. (2009) *Theory of Elastic Stability*, Courier Corporation: Dover Ed. New York.

12 Sadik, S. and Yavari, A. (2014) Geometric nonlinear thermoelasticity and the time evolution of thermal stresses. *Math. Mech. Solids*, **19**, 135–151.

13 Sadik, S., Angoshtari, A., Goriely, A. and Yavari, A. (2016) A geometric theory of nonlinear morphoelastic shells. *J Nonlin. Sci.*, **26**, 929–978.

14 Saif, M. T. A., Hui, C. Y. and Zehnder, A. T. (1993) Interface shear stresses induced by non-uniform heating of a film on a substrate. *Thin Solid Films*, **224**, 159–167.

15 McDowell, D. L. (1997) An approximate algorithm for elastic-plastic two-dimensional rolling/sliding contact. *Wear*, **211**, 237–246.

16 Yadroitsev, I. and Yadroitsava, I. (2015) Evaluation of residual stress in stainless steel 316L and Ti6Al4V samples produced by selective laser melting. *Virtual Phys. Prototot.*, **10**, 67–76.

17 Fergani, O., Jiang, X., Shao, Y., Welo, T., Yang, J. and Liang, S. (2016) Prediction of residual stress regeneration in multi-pass milling. *Int. J. Adv. Man.Tech.*, **83**, 1153–1160.

18 Scott-Emuakpor, O., Schwartz, J., George, T., Holycross, C., Cross, C. and Slater, J. (2015) Bending fatigue life characterisation of direct metal laser sintering nickel alloy 718. *Fatigue Fract. Eng. Mater. & Struct.*, **38**, 1105–1117.

19 Croccolo, D., De Agostinis, M., Fini, S., Olmi, G., Vranic, A. and Ciric-Kostic, S. (2016) Influence of the build orientation on the fatigue strength of EOS maraging steel produced by additive metal machine. *Fatigue Fract. Eng. Mater. & Struct.*, **39**, 637–647.

20 Edwards, P. and Ramulu, M. (2015) Effect of build direction on the fracture toughness and fatigue crack growth in selective laser melted Ti–6Al–4V. *Fatigue Fract. Eng. Mater. & Struct.*, **38**, 1228–1236.

21 Lauwers, B., Klocke, F., Klink, A., Tekkaya, A. E., Neugebauer, R. and Mcintosh, D. (2014) Hybrid processes in manufacturing. *CIRP Ann. Manuf. Technol.*, **63**, 561–583.

22 Yamaguchi, H. and Shinmura, T. (1999) Study of the surface modification resulting from an internal magnetic abrasive finishing process. *Wear*, **225–229**, 246–255.